

PAPER • OPEN ACCESS

Unsteady MHD blood flow through porous medium in a parallel plate channel

To cite this article: R Latha and B Rushi Kumar 2017 *IOP Conf. Ser.: Mater. Sci. Eng.* **263** 062020

View the [article online](#) for updates and enhancements.

Related content

- [Heat and mass transfer effect on MHD natural convection flow past a moving vertical plate](#)
Siva Reddy Sheri and J Anand Rao
- [Simulation Analysis and Experimental Verification of LIGA-Like Process for Ni-Fe Micromold Insert with Taper Angle](#)
Ming-Nan Fu, Yih-Min Yeh and George-Chia Tu
- [Numerical Simulation of and Experiment on Electroforming Microstructure Mold Insert](#)
Ming-Nan Fu

Unsteady MHD blood flow through porous medium in a parallel plate channel

R Latha and B Rushi Kumar

Department of Mathematics, School of Advanced Sciences, VIT University, Vellore-632 014, India

E-mail: rushikumar@vit.ac.in

Abstract. In this study, we have analyzed heat and mass transfer effects on unsteady blood flow through parallel plate channel in a saturated porous medium in the presence of a transverse magnetic field with thermal radiation. The governing higher order nonlinear PDE'S are converted to dimensionless equations using dimensionless variables. The dimensionless equations are then solved analytically using boundary conditions by choosing the axial flow transport and the fields of concentration and temperature apart from the normal velocity as a function of y and t . The effects of different pertinent parameters appeared in this model viz thermal radiation, Prandtl number, Heat source parameter, Hartmann number, Permeability parameter, Decay parameter on axial flow transport and the normal velocity are analyzed in detail.

1. Introduction

The development of flow models in porous media has a bearing on the progress of several applications like transport of macromolecules in aortic media, blood flow through contracting muscles etc. The porous medium is a solid body that contains pores. The flow of fluid through pores, these pores are not like straight through, they are not going to be circular and they have many channels. The porous medium has very fine holes, fluid is not flowing through solid, and it is only flowing through the open edge. The characteristic of porosity has much concentrated of specialist why because it has various applications in the biological fluid such as human lungs, vascular beds, kidney, and bone etc. The porous medium is more related to Darcy's law, it is depicted that proportionality between the flow velocity and the pressure difference for low speed in an unbounded porous medium. Porous medium modeling has been applied not only at the tissue level but also at the organ level. For example, the lung, under SEM investigation appears like a sponge with anatomic complexity including multiple bifurcations and microscopic cavities making it a classic porous medium. The airflow and gas exchanges within a lung may be considered examples of fluid flow through a porous medium.

Mortimer et al. [1], Ramamurthy et al. [2], Mustapha et al. [3] and Mekheimer [4] are investigated the MHD effects on blood flow takes place through a porous medium. A porous structure is formed by fatty substances, blood clots, and cholesterol. Jha et al. [5] and Lai et al. [6] are examined mass transfer and free convection in the blood flow through a porous medium. In this situation, the permeability parameter is assumed to be constant. Mohamed Ismail et al. [7] and Ganesh et al. [8] are examined the problem for unsteady MHD Blood flow of viscous fluid between parallel porous plates.



Barcroft et al. [9] presented in the paper which enable a more rational choice of water bath temperature to be made by comparing the temperature of the skin, subcutaneous tissue and muscle, and the blood flow of the whole forearm, in the clothed forearm and when the arm is immersed in water at different temperatures. Kolin [10] only first examined the idea of an electromagnetic flow and its application to blood flow measurements in medical research and later the work is extended by Korchevskii et al. [11]. The blood flow in the large arteries in the presence of a homogeneous magnetic field was examined by Vardanyan [12]. Srinivas et al. [13] and [14] and Kothandapani [15] are studied the effect of heat transfer and magnetic field in the peristaltic flow. Charny [17] investigated the peristaltic flow of thermal regulation. ArunnNarasimhan [16] studied the role of porous medium modeling in bio thermal fluids and he concluded that the potential of the more advanced bio-heat transfer models formulated using porous medium concepts of local thermal non-equilibrium between the tissue and blood flow, is yet to be fully realized. Becker [18] investigated thermodynamic based on the model of skin electroporation. Rathod et al. [19] studied ureteral peristalsis in the cylindrical tube through a porous medium and concluded the peristaltic transport of a viscous incompressible fluid through a porous medium using the geometrical form of the ureter. Sharma et al. [20] investigated two-dimensional heterogeneous porous media with finite difference method resulted in a higher virus concentration. Anand et al. [21] studied MHD dusty fluid flow of an exponentially stretching sheet with heat dissipation over porosity. Chandra Sekar et al. [22] examined MHD blood flow of heat dissipation through porous space. Kirubhashankar et al. [23] investigated Casson fluid flow and heat transfer over an unsteady porous stretching surface.

Here blood treated as a viscous, electrically conducting and incompressible fluid. We analyzed the unsteady hydro magnetic flow of blood past a parallel plate channel over a porous medium. We also incorporated the thermal radiation of the heat transfer in the fluid. In the present paper, we examine the unsteady hydro magnetic blood flow with heat and mass transfer and blood flow passes through a porous medium in a biological state where the lumen of the blood vessel segment is turned into porous structure due to the accumulation of fats, cholesterol, and blood clots. The motivation of present analysis has the promise of important application in electromagnetic therapy, which has gained much popularity in the treatment of cancer. In order to estimate the flow transport, temperature and mass concentration for different values of Prandtl number (Pr), Radiation parameter (R), Hartmann number (Ha), Schmidt number (Sc), Heat source parameter (N). The governing partial differential equations are solved by using the analytic method.

2. Formulation and solution of the problem

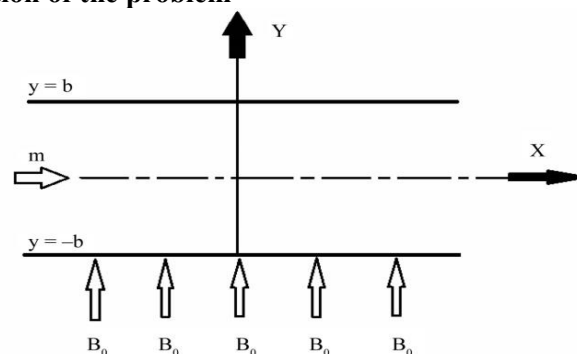


Figure 1. Geometry of the problem

We assume that the blood flows in the porous medium to be Newtonian, incompressible, viscous homogeneous fluid and viscosity of the blood to be constant. In this model, we considered the effect of the magnetic field which is applied in a direction perpendicular to the blood flow. Considering u and v are velocity components in x-axis and y-axis respectively at time t . we have to write the boundary layer equations as,

$$\frac{\partial u}{\partial x} + \frac{\partial v}{\partial y} = 0 \quad (1)$$

$$\frac{\partial u}{\partial t} + \frac{1}{\rho} \frac{\partial p}{\partial x} = \frac{\mu}{\rho} \frac{\partial^2 u}{\partial y^2} - \frac{\sigma B_0^2 u}{\rho} - \frac{vu}{k} + g\beta(T - T_0) + g\beta^*(C - C_0) \quad (2)$$

$$\frac{\partial T}{\partial t} = \frac{K'}{\rho C_p} \frac{\partial^2 T}{\partial y^2} + \frac{Q}{\rho C_p} (T - T_0) - \frac{1}{\rho C_p} \frac{\partial q_r}{\partial y} \quad (3)$$

$$\frac{\partial C}{\partial t} = D \frac{\partial^2 C}{\partial y^2} - K_r (C - C_0) \quad (4)$$

By using Rosseland's approximation, the thermal radiation heat flux q is given by,

$$q = \frac{-4\sigma^* \partial T^4}{3k^* \partial r} \quad (5)$$

Where σ^* is the Stefan-Boltzmann constant and k^* is the mean absorption coefficient, if the difference of temperature is small, then equation (5) can be linearized by expanding T^4 into Taylor series about T_0 (T_0 is the wall temperature) after neglecting higher order terms takes the form

$$T^4 \cong 4T_0^3 T - 3T_0^4 \quad (6)$$

Substituting Taylor expansion, the radiation heat flux q can be expressed as

$$q = \frac{-4\sigma^* \partial(4T_0^3 T - 3T_0^4)}{3k^* \partial r}$$

Hence equation (3) becomes

$$\frac{\partial T}{\partial t} = \frac{1}{\text{Pr}} \frac{\partial^2 T}{\partial y^2} + \frac{QTb^2}{k \text{Pr}} + \frac{16\sigma^* T_0^3}{3kk^* \text{Pr}} \frac{\partial^2 T}{\partial y^2}$$

Introducing the following non dimensional variables

$$x^* = \frac{x}{h}, y^* = \frac{y}{h}, u^* = \frac{u}{m/2\rho h}, v^* = \frac{v}{m/2\rho h}, t^* = \frac{t}{\rho h^2/\mu}, \quad (7)$$

$$P^*(x, t) = \frac{dp/dx}{\mu m/2\rho h^3}, \theta^* = \frac{\theta}{\mu m/2\rho^2 h^3}, C^* = \frac{C}{\mu m/2\rho^2 h^3}, M = \frac{\sigma B_0^2 h^2}{\mu},$$

$$N = \frac{Qh^2}{K}, \text{Pr} = \frac{\mu C_p}{K}, \text{Cr} = \frac{K_r h^2}{v}, \text{Sc} = \frac{v}{D}, R = \frac{16\sigma^* T_0^3}{3kk^*}$$

Substituting equation (7) into the equations (1) - (4) we get the following equations after dropping the stars as

$$\frac{\partial u}{\partial x} + \frac{\partial v}{\partial y} = 0 \quad (8)$$

$$\frac{\partial u}{\partial t} + p = \frac{\partial^2 u}{\partial y^2} - Ha^2 u - \frac{h^2 u}{k} + g\beta\theta + g\beta^* C \quad (9)$$

$$\frac{\partial \theta}{\partial t} = \frac{(1+R)}{\text{Pr}} \frac{\partial^2 \theta}{\partial y^2} + \frac{N\theta}{\text{Pr}} \quad (10)$$

$$\frac{\partial C}{\partial t} = \frac{1}{\text{Sc}} \frac{\partial^2 C}{\partial y^2} - CCr \quad (11)$$

From equation (10) we notice that the temperature θ has the first derivative with respect to time t . Hence the solution of PDE by variables separable techniques we get the following equation

The expression of temperature can be written as

$$\theta = e^{-\lambda^2 t}$$

The boundary conditions are taken as

$$u = e^{-\lambda^2 t}, \theta = e^{-\lambda^2 t}, C = e^{-\lambda^2 t} \quad \text{at } y = -1$$

$$u = 0, \theta = 0, C = 0 \quad \text{at } y = 1 \quad (12)$$

The solutions of the equation (8)-(11) respectively as

$$u(y, t) = F(y)e^{-\lambda^2 t} \quad (13)$$

$$v(y, t) = G(y)e^{-\lambda^2 t} \quad (14)$$

$$\theta(y, t) = H(y)e^{-\lambda^2 t} \quad (15)$$

$$C(y, t) = I(y)e^{-\lambda^2 t} \quad (16)$$

Substituting from equations (13) - (16) into equations (8)-(12) we obtain the following equations,

$$\frac{\partial^2 F}{\partial y^2} + F\delta^2 = P - g\beta H - g\beta^* I \quad (17)$$

$$\text{Where } \delta = \sqrt{\lambda^2 - Ha^2 - \frac{h^2}{k}} \text{ and } P = \frac{p}{e^{-\lambda^2 t}}$$

$$G = C \quad (a \text{ constant}) \quad (18)$$

$$\frac{\partial^2 H}{\partial y^2} + \left(\frac{N + \lambda^2 \text{Pr}}{1 + R} \right) H(y) = 0 \quad (19)$$

$$\frac{\partial^2 I}{\partial y^2} + \text{Sc}(\lambda^2 - Cr) I(y) = 0 \quad (20)$$

The boundary conditions as follows

$$F = 1, H = 1, I = 1, \quad \text{at } y = -1$$

$$F = 0, H = 0, I = 0, \quad \text{at } y = 1 \quad (21)$$

The equations (19) and (20) as follows

$$H(y) = c_1 \cos(\alpha y) + c_2 \sin(\alpha y) \quad (22)$$

$$I(y) = d_1 \cos(\xi y) + d_2 \sin(\xi y) \quad (23)$$

$$\text{Where } \alpha = \sqrt{\left(\frac{N + \lambda^2 \text{Pr}}{1 + R} \right)}, \xi = \sqrt{\text{Sc}(\lambda^2 - Cr)}$$

Using the boundary conditions (21) we observe

$$c_1 = \frac{1}{2 \cos \alpha} \quad \text{and} \quad c_2 = \frac{-1}{2 \sin \alpha}$$

$$d_1 = \frac{1}{2 \cos \xi} \quad \text{and} \quad d_2 = \frac{-1}{2 \sin \xi}$$

Then the final form of $H(y)$ and $I(y)$ are,

$$H(y) = \frac{1}{2 \cos \alpha} \cos(\alpha y) - \frac{1}{2 \sin \alpha} \sin(\alpha y) \quad (24)$$

$$I(y) = \frac{1}{2 \cos \xi} \cos(\xi y) - \frac{1}{2 \sin \xi} \sin(\xi y) \quad (25)$$

From equations (15), (16), (24) and (25) the temperature and concentration profile is

$$\theta(y, t) = \left(\frac{1}{2 \cos \alpha} \cos(\alpha y) - \frac{1}{2 \sin \alpha} \sin(\alpha y) \right) e^{-\lambda^2 t} \quad (26)$$

$$C(y, t) = \left(\frac{1}{2 \cos \xi} \cos(\xi y) - \frac{1}{2 \sin \xi} \sin(\xi y) \right) e^{-\lambda^2 t} \quad (27)$$

Using equation (24) and (25) into equation (17) becomes,

$$F''(y) + F(y)(\lambda^2 - Ha^2 - \frac{h^2}{k}) = P - g\beta \left(\frac{1}{2 \cos \alpha} \cos(\alpha y) - \frac{1}{2 \sin \alpha} \sin(\alpha y) \right) - g\beta^* \left(\frac{1}{2 \cos \xi} \cos(\xi y) - \frac{1}{2 \sin \xi} \sin(\xi y) \right) \quad (28)$$

Solving equation (28) to obtain the homogeneous solution of F using equation (21) as follows

$$F_h = B_1 \cos(\delta y) + B_2 \sin(\delta y)$$

Using the boundary condition (21) we observe

$$B_1 = \frac{1 - 2B_3 + 2B_4 \cos \alpha + 2B_6 \cos \xi}{2 \cos \delta}$$

$$B_2 = \frac{1 + 2B_5 \sin \alpha + 2B_7 \sin \xi}{-2 \sin \delta}$$

The particular solution is

$$F_p = B_3 - B_4 \cos(\alpha y) + B_5 \sin(\alpha y) - B_6 \cos(\xi y) + B_7 \sin(\xi y) \quad (29)$$

The general solution of F is

$$F = B_1 \cos(\delta y) + B_2 \sin(\delta y) + B_3 - B_4 \cos(\alpha y) + B_5 \sin(\alpha y) - B_6 \cos(\xi y) + B_7 \sin(\xi y) \quad (30)$$

From equation (13) and (29) the axial flow transport becomes

$$u(y,t) = (B_1 \cos(\delta y) + B_2 \sin(\delta y) + B_3 - B_4 \cos(\alpha y) + B_5 \sin(\alpha y) - B_6 \cos(\xi y) + B_7 \sin(\xi y))e^{-\lambda^2 t} \quad (31)$$

Where

$$B_3 = \frac{P}{\delta^2}, B_4 = \frac{g\beta}{2\cos\alpha(\delta^2 - \alpha^2)}, B_5 = \frac{g\beta}{2\sin\alpha(\delta^2 - \alpha^2)},$$

$$B_6 = \frac{g\beta^*}{2\cos\xi(\delta^2 - \xi^2)}, B_7 = \frac{g\beta^*}{2\sin\xi(\delta^2 - \xi^2)}$$

From equations (14) and (18) the normal velocity becomes,

$$v(y,t) = Ce^{-\lambda^2 t} \quad (32)$$

Where C is arbitrary constant ($C=1$) the equations (26), (27), (31) and (32) are the temperature, concentration, axial flow transport and normal velocity respectively.

3. Results and Discussion

The blood flow examination has been carried out to analyze the influence of Hartmann number, permeability parameter, heat source parameter and Prandtl number. The numerical computation is done in MATLAB and computational results are presented graphically.

3.1. Effect on different physical parameters on axial velocity profiles

Figure 2-5 reveals the axial velocity for various values of N , K , Ha and t at $\lambda=0.5$, $\rho=0.5$, $R=0.5$, $h=0.5$, $Pr=1$, $\beta=0.5$, $\beta^*=0.5$, $g=9.81$, $Sc=1$, $Cr=0.8$, $p=0.5$. As shown from Figure 2, axial velocity enhances as heat source parameter enhances. It means that the velocity boundary layer thickness increases for large values of N , moreover, the maximum values of the velocity are 1.6590, 1.7667, 1.9017, 2.0762 and 2.3104 for $N=1, 1.25, 1.5, 1.75$ and 2 respectively at each of which occurs at $y=-0.2$. It is noticed that the velocity increases by 39.264% when N increases from 1 to 2. From Figure 3 Axial velocity enhances permeability parameter k enhances and the maximum values of the velocity are 1.0756, 1.3803, 1.5227, 1.6052 and 1.6590 for $k=0.1, 0.2, 0.3, 0.4$ and 0.5 respectively at each of which occurs at $y=-0.2$. It is observed that the velocity increases by 54.239% when k increases from 0.1 to 0.5. But from Figure 4, axial velocity diminishes as Hartmann number Ha enhances, furthermore, the maximum values of the velocity are 2.0752, 1.8791, 1.6590, 1.4410 and 1.2404 for $Ha=0.5, 0.75, 1, 1.25$ and 1.5 respectively at each of which occurs at $y=-0.2$. It is noticed that the velocity decreases by -40.227% when Ha increases from 0.5 to 1.5. From Figure 5, axial velocity diminishes as t enhances, moreover the maximum values of the velocity are 0.7788, 0.6065, 0.4724, 0.3679 and 0.2865 for $t=1, 2, 3, 4$ and 5 respectively at each of which occurs at $y=-1$. It is noticed that the velocity decreases by -63.212% when t increases from 1 to 5. That is permeability increases as the pores increase as well as the axial velocity enhances and are easily permeated the blood. So the blood quickly purified as well as lungs are improving blood circulation and make the man healthier. Lungs are made up of tiny round spongy sacs, called alveoli sacs. These expand during inhalation and the oxygen to be absorbed into the blood. Pollutants destroy the elasticity of the alveoli sacs and many of them get destroyed also to cancer. Lack of rich oxygen supply to the body affects all systems adversely.

3.2. Effect on different physical parameters on temperature profiles

Figure 6-8 reveals the temperature distribution for various values of R , Pr and N at $t=1$, $\lambda=0.5$, $\rho=0.5$, $Ha=0.5$, $h=0.5$, $\beta=0.5$, $\beta^*=0.5$, $g=9.81$, $Sc=1$, $Cr=0.8$, $p=0.5$, $k=0.5$. It is noticed that from Figure 7 the temperature enhances with enhancing values of Prandtl number Pr . Moreover, the maximum values of the temperature are 0.7156, 0.7983, 0.9018, 1.0353 and 1.2142 for $Pr=1, 2, 3, 4$ and 5 respectively at each of which occurs at $y=-0.2$. It is noticed that the temperature enhances by 69.675% when Pr increases from 1 to 5. From Figure 8 the temperature enhances with enhancing values of Heat source parameter N and the maximum values of the temperature are 0.6802, 0.7547, 0.8470, 0.9640 and 1.1177 for $N=1, 1.25, 1.50, 1.75$ and 2 respectively at each of which occurs at $y=-0.2$. It is observed that the temperature increases by 64.319% when N increases from 1 to 2. From Figure 6 the temperature diminishes with enhancing values of R . Furthermore, the maximum values of the temperature are 0.7156, 0.6660, 0.6329, 0.6093 and 0.5916 for $R=0.5, 0.75, 1, 1.25$ and 1.5 respectively at each of which occurs at $y=-0.2$. It is noticed that the temperature reduces by -17.328% when R increases from 0.5 to 1.5.

3.3. Effect on different physical parameters on concentration profiles

Figure 9-10 shows that the concentration distribution for various values of Sc and Cr at $t=1$, $\lambda=0.5$, $\rho=0.5$, $Ha=0.5$, $h=0.5$, $R=0.5$, $\beta=0.5$, $\beta^*=0.5$, $g=9.81$, $Pr=0.5$, $p=0.5$, $N=1$, $k=0.5$. It is noticed that from Figure 9 the concentration distribution decreases as Sc (Schmidt number) increases and maximum values of the concentration are 0.3771, 0.2675, 0.2031, 0.1607 and 0.1307 for $Sc=1, 3, 5, 7$ and 9 respectively at each of which occurs at $y=-0.2$. It is observed that the concentration decreases by -65.340% when Sc increases from 1 to 9. From Figure 10 the concentration distribution reduces as Cr (Chemical reaction parameter) increases. Furthermore, maximum values of the concentration are 0.3771, 0.2751, 0.2127, 0.1707 and 0.1405 for $Cr=0.8, 1.8, 2.8, 3.8$ and 4.8 respectively at each of which occurs at $y=-0.2$. It is observed that the concentration decreases by -62.741% when Cr increases from 0.8 to 4.8.

3.4. Effect on different physical parameters on normal velocity

Figure 11 shows that the normal velocity for different values of λ at $\rho=0.5$, $Ha=0.5$, $h=0.5$, $R=0.5$, $\beta=0.5$, $\beta^*=0.5$, $g=9.81$, $Pr=0.5$, $p=0.5$, $N=1$, $k=0.5$. It is noticed that normal velocity decreases as λ enhances and maximum values of the normal velocity are 0.1653, 0.0863, 0.0408 and 0.0174 for $\lambda=1.5, 1.75, 2$ and 2.25 respectively at each of which occurs at $y=-0.2$. It is noticed that the normal velocity reduces by -89.473% when λ increases from 1.5 to 2.25.

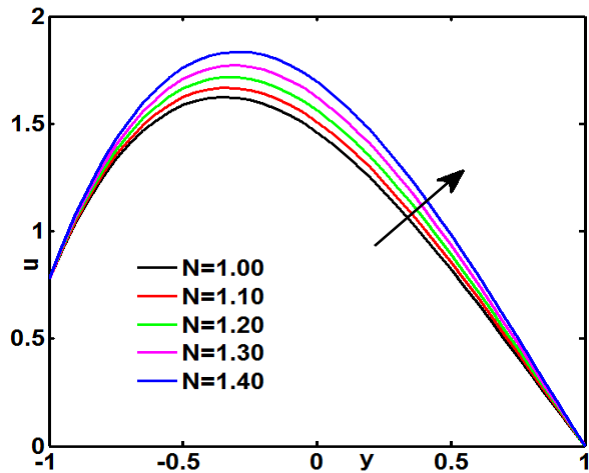


Figure 2. Axial velocity for various values of N when $k = 0.5, Ha = 1$

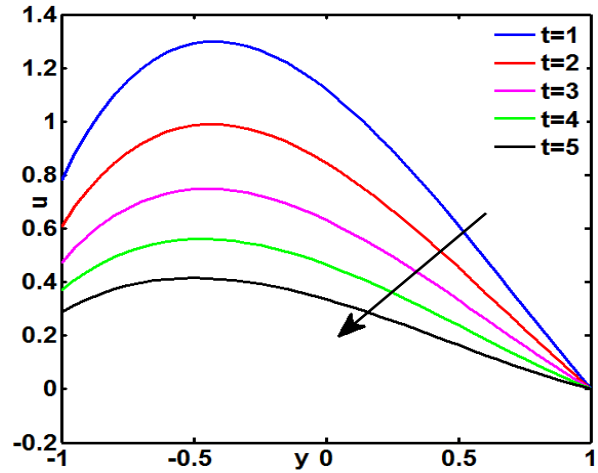


Figure 5. Axial velocity for different t when $k = 0.5, Ha = 1, N = 1$

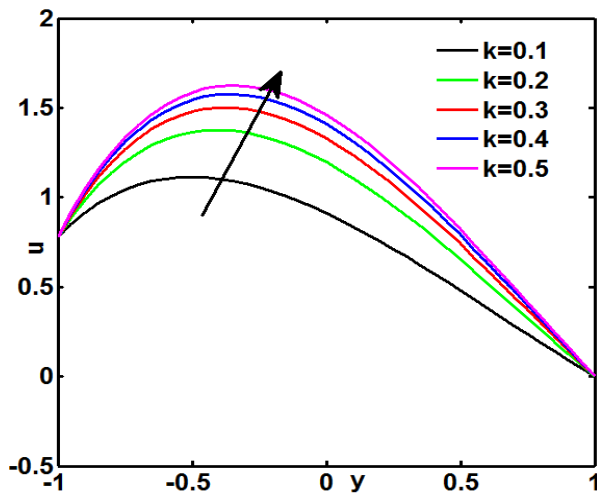


Figure 3. Axial velocity for different k when $Ha = 1, N = 1$

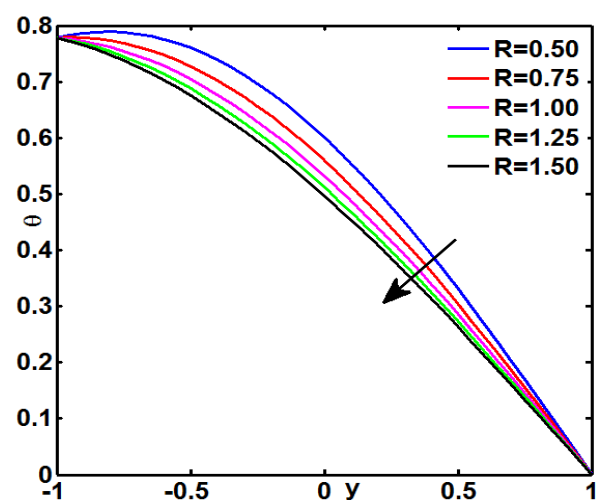


Figure 6. Temperature distribution for various R when $Pr = 1, N = 1$

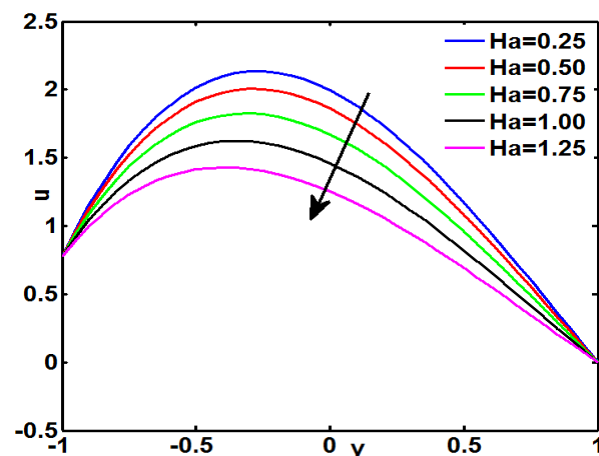


Figure 4. Axial velocity for different k when $Ha = 1, N = 1$

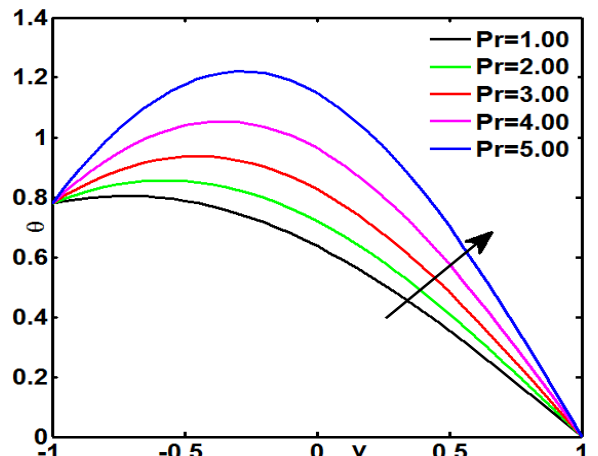


Figure 7. Temperature distribution for different Pr when $R = 0.5, N = 1$

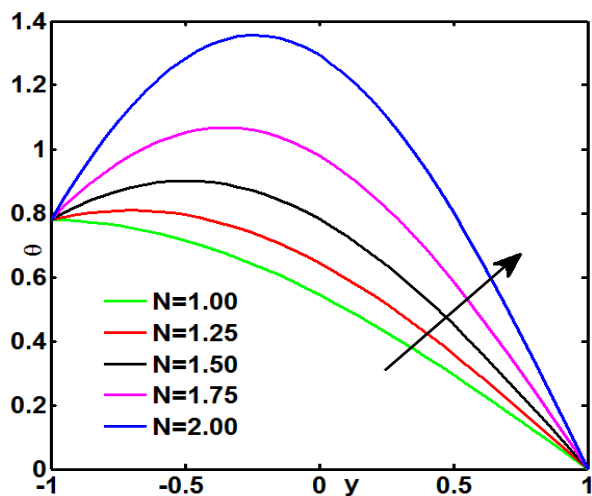


Figure 8. Temperature distribution for different N when $R=0.5$, $Pr=0.5$.

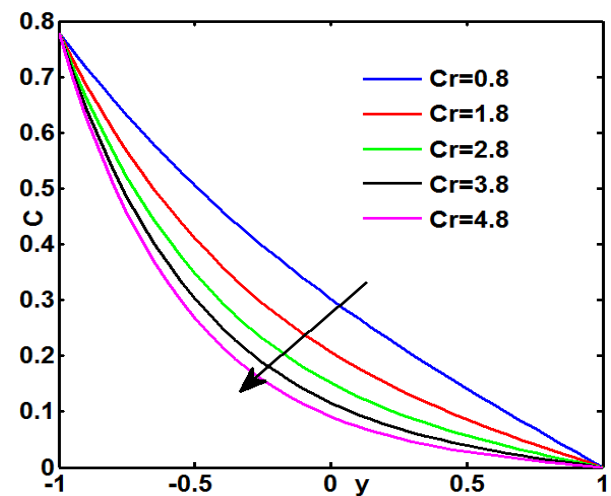


Figure 10. Concentration distribution for different Cr when $Sc=0.5$.

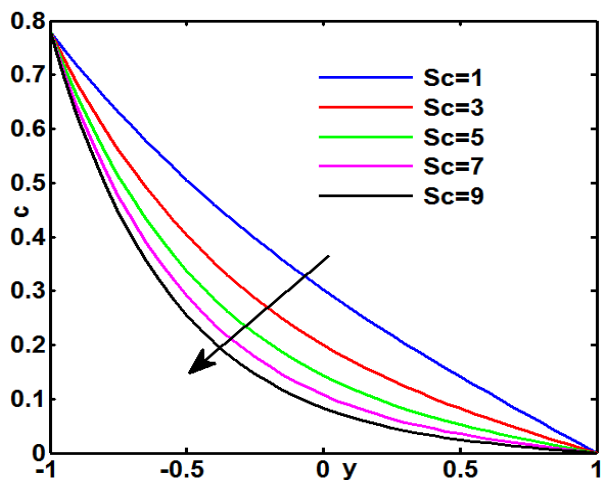


Figure 9. Concentration distribution for different Sc when $Cr=0.8$.

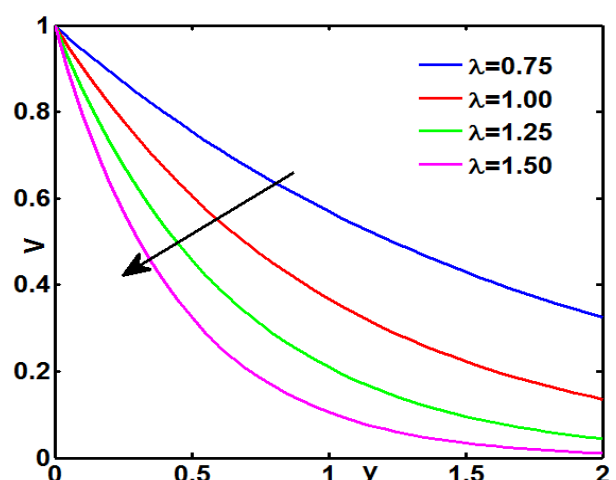


Figure 11. Normal velocity distribution for different λ .

4. Conclusions

A theoretical investigation has been carried out for unsteady blood flow through a porous medium in a constricted porous channel subjected to heat source and radiation. Also, the study investigates the effect of Hartmann number and permeability parameter on blood flow through a parallel plate channel. The prime concern in our present study has been to assess the role of axial flow transport in blood flow through a parallel plate channel and to determine those regions where the axial velocity is low. Thus, the study bears the potential for further exploration of the causes and development of arterial diseases. From the computational results, it may be concluded that:

- Axial velocity enhances with enhancing values of the permeability parameter k and heat source parameter N .
- Axial velocity diminishes with enhancing values of the Hartmann number Ha .
- Temperature enhances with enhancing values of the heat source parameter N and Prandtl number Pr .
- Temperature diminishes with enhancing values of the radiation.

- Concentration diminishes with enhancing values of Schmidt number Sc and chemical reaction parameter Cr .

References

- [1] Mortimer R G and Eyring H 1980 *Proc. Nat. Acad. Sci.* **77** 1728–1731
- [2] Ramamurthy G and Shanker B 1994 *Med. Biol. Eng. Comput.* **32** 655–659
- [3] Mustapha M, Amin N, Chakravarty S and Mandal P K 2009 *Comput. Biol. Med.* **39** 896–906
- [4] Mekheimer K S 2004 *Appl. Math. Comput.* **153** 763–777
- [5] Jha B K and Prasad R 1992 *J. Math. Phys. Sci.* **26** 1–8
- [6] Lai F C 1991 *Int. Comm. Heat Mass Trans.* **18** 93–106
- [7] Mohamed Ismail A, Ganesh S and Kirubhashankar C K 2013 *International Journal on Design and Manufacturing Technologies* **7** 1–6
- [8] Ganesh S and Krishnambal S 2007 *Int. J Information Sciences and Computing* **1** 63 - 66
- [9] Barcroft H and Edholm O G 1942 *J. Physiol.* **10** 25–20
- [10] Kolin A 1936 *Proc. Soc. exp. Biol. (N. Y.)* **35** 53–56
- [11] Korchevskii E M and Marochnik L S 1965 *Biophysics* **10** 411–413
- [12] Vardanyan V A 1973 *Biophysics* **18** 515–521
- [13] Srinivas S, Gayathri R and Kothandapani M 2009 *Comput. Phys. Commun.* **180** 2115–2122
- [14] Srinivas S and Kothandapani M 2009 *Appl. Math. Comput.* **213** 197–208
- [15] Kothandapani M and Srinivas S 2008 *Int. J. Non-linear Mech.* **43** 915–924
- [16] Arunn Narasimhan 2011 *Journal of the Indian Institute of Science* **91** 243–266
- [17] Charny C K 1992 Academic Press Inc., Boston, USA, *Ch. Advances in Heat Transfer* 19–156
- [18] Becker S M 2011 *Journal of Heat Transfer* **133** 1–9
- [19] Rathod V and Channakote M 2011 *Advances in Applied Science Research* **2** 134–140
- [20] Sharma P K and Srivastava R 2011 *Journal of Hydro-environment Research* **5** 93–99
- [21] Anand V W J, Ganesh S, Mohamed Ismail A and Kirubhashankar C K 2015 *Applied Mathematical Sciences* **9** 2083 – 2090
- [22] Chandra Sekar P, Ganesh S, Mohamed Ismail A and Kirubhashankar C K 2015 *Applied Mathematical Sciences* **9** 1509 – 1516
- [23] Kirubhashankar C K, Ganesh S and Mohamed Ismail A 2015 *Applied Mathematical Sciences* **9** 345 – 351